Future Foods 14 (2026) 101098

Contents lists available at ScienceDirect

Future Foods

journal homepage: www.elsevier.com/locate/fufo

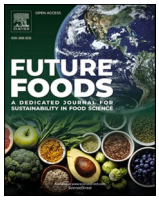

Effects of hempseeds on cell viability and proliferation in 2D and 3D culture systems: Implications for cellular agriculture

D. Lanzoni [a,1], G. Zanderigo [b,1], S. Nonnis [a,e], G. Tedeschi [a,e], B.M. Colosimo [b], S. Gioria [c,*], T.S. Sundaram [a], P.A. Corsetto [d], F. Cheli [a,e], C. Giromini [a,f]

[a] Department of Veterinary Medicine and Animal Science, University of Milan, Via dell'Università 6, 26900 Lodi, Italy
[b] Department of Mechanical Engineering, Politecnico di Milano, Via La Masa 1, 202156 Milano, Italy
[c] European Commission, Joint Research Centre (JRC), Ispra, Italy
[d] Department of Pharmacological and Biomolecular Sciences "Rodolfo Paoletti", University of Milan, Via Balzaretti 9, 20133 Milan, Italy
[e] CRC, Innovation for Well-Being and Environment, Università degli Studi di Milano, 20122 Milano, Italy
[f] Institute for Food, Nutrition and Health, University of Reading, Reading RG6 5EU, UK

ARTICLE INFO

Keywords:
Alternative proteins
Cultured media
Sustainable production
Hempseed
3D-bioprinting

ABSTRACT

The growing interest in cultured meat (CM) highlights the urgent need for sustainable and ethically acceptable culture media, particularly alternatives to animal-derived ingredients. In this study, we evaluated hempseed protein isolate (HSPI) as a functional supplement in both 2D and 3D cell culture systems using murine C2C12 muscle cells. Proteomic and peptidomic analyses identified 231 proteins and more than 500 endogenous peptides, including several bioactive sequences with antioxidant, ACE-inhibitory, and immunomodulatory properties.

In 2D cultures, HSPI at 0.01 mg/mL supported cell viability at 24 h (110.10 ± 3.33%) and 48 h (118.93 ± 2.66%), with values comparable to the FBS control (117.83 ± 3.64% and 121.62 ± 0.81%, respectively). Morphological observations, together with the expression of Cyclin D1 and Cyclin-Dependent Kinase 4, confirmed that HSPI was able to sustain cell proliferation. Long-term supplementation in 2.5% FBS did not significantly affect cell proliferation before or after cryopreservation over a one-month period; however, it significantly increased the total antioxidant activity in cell lysates.

In 3D-bioprinted constructs, HSPI maintained high cell viability over seven days when either added to the culture medium or incorporated directly into the bioink. Notably, HSPI incorporated into the bioink preserved cell viability at levels comparable to FBS even at day 7. Overall, these findings suggest that HSPI represents a promising plant-based ingredient for CM culture media, while simultaneously enhancing the antioxidant profile of cultured cells, highlighting its potential application in the development of functionalized cell-based products.

1. Introduction

Cultured meat (CM) is rapidly emerging as a promising alternative to conventional meat, aiming to reduce the environmental impact of the food sector (Vermeulen et al., 2012; Lindgren et al., 2018; Benton et al., 2021), improve animal welfare and meet the growing global demand for protein. Starting with the expansion and differentiation of animal cells under controlled conditions, CM has the potential to radically transform the agri-food sector, providing products similar to traditional meat in terms of composition and organoleptic properties, but obtained without intensive farming or slaughter (Post, 2012; Eibl et al., 2021).

However, for this technology to become economically competitive and sustainable on a large scale, several scientific and technological challenges need to be addressed and overcome (Lanzoni et al., 2022). Among these, one of the most relevant is the composition and cost of the cell culture medium, which is not only the main cost item in CM production, but also a critical issue in terms of ethics, sustainability and safety (Stout et al., 2023; World Health Organization, 2023; Lanzoni

* Corresponding author.
E-mail address: Sabrina.GIORIA@ec.europa.eu (S. Gioria).
[1] These authors contributed equally.

https://doi.org/10.1016/j.fufo.2026.101098
Received 26 September 2025; Received in revised form 9 March 2026; Accepted 18 June 2026
Available online 19 June 2026
2666-8335/© 2026 Published by Elsevier B.V. This is an open access article under the CC BY-NC-ND license (http://creativecommons.org/licenses/by-nc-nd/4.0/).

et al., 2024; Formici et al., 2026).

The culture medium supplies the cells with all the nutrients they need for survival, proliferation and differentiation: amino acids, sugars, vitamins, salts, lipids, but also a range of bioactive factors such as hormones, growth factors, carrier proteins and other regulatory molecules (Hubalek et al., 2022). However, nowadays, many cell culture protocols involve the use of components of animal origin, commonly employed to ensure an adequate supply of nutrients, growth factors and other biomolecules essential for cell survival, proliferation and differentiation (Sundaram et al., 2025). Of these, foetal bovine serum (FBS) represents one of the most widely used sources. Other supplements and additives derived from animal tissue also contribute significantly to the composition of conventional media.

Although these components are biologically effective, their animal origin and the methods of obtaining them pose significant ethical and animal welfare issues (Chelladuray et al., 2021). In addition, the use of animal ingredients is associated with critical issues such as high variability between batches, the risk of organic contamination, high costs and a structural dependence on conventional farming systems, the same ones that cellular agriculture intends to progressively overcome (Lanzoni et al., 2022).

For this reason, scientific and industrial research is increasingly directed towards the development of culture media free of animal components (Ho et al., 202X). Current efforts focus on the identification and functional replacement or reduction of individual components of FBS, which are known to play essential roles in maintaining cell viability and function (Stout et al., 2023). Plant-derived proteins and hydrolysates are being investigated as sustainable alternative ingredients that can replicate these functions while enabling ethical and scalable production. A recent example is provided by Stout et al. (2023), who reported the use of hydrolysates obtained from cottonseed, rapeseed, Inca peanut, and soybean to support cell growth in the context of CM.

In this context, among oilseeds, hempseeds (HSs, *Cannabis sativa* L.) represent a particularly promising solution. Particularly, the cultivation of hemp not only meets established criteria of environmental sustainability, due to its low need for agronomic inputs and ability to improve soil quality but is also widely valued for its nutritional and biochemical profile (Farinon et al., 2020; Lanzoni et al., 2023). Specifically, HSs contain approximately 25-35% lipids, characterised by a high content of polyunsaturated fatty acids, particularly omega-3 and omega-6, present in a physiologically optimal ratio and a significant source of crude protein (23-30%), featured by high biological value (Farinon et al., 2020; Lanzoni et al., 2023). The favourable nutritional profile of HSs, alongside their relevant functional properties (Farinon et al., 2020; Lanzoni et al., 2023), has prompted increasing scientific interest in their application within the nutritional sector. Nevertheless, to the best of our knowledge, no studies have so far explored the use of HSs as an alternative ingredient for the formulation of culture media intended for cellular agriculture applications.

For this reason, in the present study, we investigated the potential of hempseed protein isolate (HSPI), obtained *via* alkaline extraction followed by isoelectric precipitation, to support both short-term viability and long-term cellular proliferation. Short-term effects on C2C12 cell viability were assessed at 24 and 48 h, while long-term proliferation was monitored up to one month. The experimental design included a two-weeks cryopreservation phase, a critical step for preserving cellular stability and functionality, to assess whether HSPI pre-treatment influences post-thaw viability and proliferative capacity. At the conclusion of the expansion period, cells were evaluated for total protein content and antioxidant capacity to identify treatment-induced biochemical alterations. Finally, HSPI was used not only as a supplement to the culture media but also as a component of a bio-ink for 3D bioprinting, allowing the assessment of its impact on cell viability within three-dimensional printed constructs.

2. Material and methods

2.1. Material

Hempseeds (*C. sativa* L., variety Futura), which chemical profile is reported in our previous study (Lanzoni et al., 2023), were kindly provided by the University of Life Sciences Prague and the Institute of Animal Sciences (Prague, Czech Republic). After harvesting, HSs were dried at 40°C to a moisture content of 7%, which is essential for proper storage. Prior to analysis, the seeds were stored in the dark at 4°C.

2.2. Methods

2.2.1. Hempseed protein isolate generation

The HSPI was obtained using an alkaline extraction followed by isoelectric precipitation, as described by Stout et al. (2023). Briefly, HSs, previously ground, were resuspended in deionised water at a 10% *w/v* ratio. The resulting suspension was alkalised to pH 12.5 by the addition of NaOH (5 M) and stirred at room temperature (RT) for 1 h. Subsequently, the mixture was centrifuged at 15,000 × g for 10 min at RT, yielding two fractions: (i) a pellet containing the insoluble components (discarded) and (ii) a supernatant containing the soluble proteins of interest. The supernatant was then acidified to pH 4.5 by the addition of HCl (6 M) to induce protein precipitation. The mixture was centrifuged again at 15,000 × g for 10 min at RT. The supernatant was discarded, while the pellet containing the precipitated proteins was resuspended in a volume of deionised water equal to the initial volume and adjusted to pH 12.5 with NaOH (5 M). To promote complete protein solubilisation, the suspension was subjected to vigorous shaking. Once a homogeneous dispersion was obtained, the pH of the solution was adjusted to 7.2 using 6 M HCl to remove any insoluble protein. The mixture was then centrifuged at 15,000 × g for 30 min at RT, and the supernatant was filtered through a 10 μm filter, then subjected to a further centrifugation at 45,000 × g at 4°C for 3 h to pellet the remaining insoluble particles. The supernatant obtained was collected and filtered through a 0.22 μm filter and freeze-dried.

2.2.2. Protein and peptidomic characterization

2.2.2.1. MS/MS proteomics methods. As described, at the end of the extraction process, the HSPI was freeze-dried prior to mass spectrometric (MS) analysis. Before MS, the freeze-dried HSPI, containing the extracted proteins, was resuspended in urea (8 M) and HEPES buffer (20 mM, pH 8.0). Protein concentration was quantified using the Bradford assay, with bovine serum albumin as the standard (Simonic et al., 1997). For proteolytic digestion, proteins were first reduced with 13 mM dithioerythritol for 15 min at 50 °C, then alkylated with 26 mM iodoacetamide for 30 min at RT in the dark. Digestion was carried out overnight (16 h at 37 °C) using sequence-grade trypsin (Sigma) at a protein-to-enzyme ratio of 20:1 (Zambonelli et al., 2003). The resulting peptides were desalted using ZipTip C18 pipette tips prior to MS analysis, following the protocols reported by Tavares et al. (2011) and Aletti et al. (2016).

Nano-HPLC-MS/MS analysis was performed using a Dionex Ultimate 3000 system coupled to a Q-Exactive Orbitrap mass spectrometer (Thermo Fisher Scientific, San Jose, CA, USA). Peptides were separated on an EASY-Spray™ capillary column (15 cm × 150 μm, 2 μm particle size, C18, 100 Å) at 35 °C, with a flow rate of 0.300 μL/min. The mobile phases consisted of: A) 0.1% formic acid in water, and B) 0.1% formic acid in 80:20 acetonitrile:water (v/v) (Bauzá-Martinez et al., 2018)

The acquired raw files were subjected to data analysis using MaxQuant (version 1.6.0.1, https://maxquant.org/). The searches were performed against the Uniprot reference *C. sativa* proteome (updated in July 2024; 30194 sequences). Trypsin was selected as the digestion enzyme, allowing for cleavage C-terminal to arginine and lysine

residues, except when followed by proline, and permitting up to two missed cleavages. Carbamidomethylation of cysteine was set as a fixed modification, while methionine oxidation, asparagine/glutamine deamidation, and N-terminal acetylation were considered as variable modifications.

A false discovery rate of 5% at the protein level was estimated by searching the MS/MS spectra against a reversed (decoy) version of the protein database. The minimum peptide length was set to 7 amino-acids, and at least one unique peptide was required for protein identification. Quantification was performed using MaxQuant's built-in label-free quantification (LFQ) algorithm, based on precursor ion intensity.

Statistical analysis of the MaxQuant output was carried out using the Perseus software platform (version 1.5.5.3). Bioinformatics analyses were conducted using Database for Annotation, Visualization and Integrated Discovery (DAVID, release 6.7) (Sherman et al., 2022) and the Kyoto Encyclopedia of Genes and Genomes (KEGG, updated March 2022; http://www.genome.jp/kegg/pathway.html). These tools were used to identify enriched biological processes, pathways, and molecular networks within the identified protein dataset. Functional annotation clustering was performed using Fisher's exact test with a significance threshold of $P \leq 0.05$. The raw mass spectrometry data have been deposited in the ProteomeXchange Consortium via the PRIDE partner repository (http://proteomecentral.proteomexchange.org) under the dataset PXD066443.

2.2.2.2. MS/MS peptidomic methods. To identify endogenous peptides, the permeate samples were analysed by peptidomic strategy by LC-nano ESI tandem mass spectroscopy, using a shotgun-label free approach, without any digestion prior to MS/MS (Aletti et al., 2016). Prior to MS analysis, the freeze-dried supernatant of HSPI was reconstituted in 0.3% (*v/v*) formic acid (Addis et al., 2020).

The peptide concentration was quantified using the Pierce Quantitative Colorimetric Peptide Assay, employing a peptide digest as the reference standard. The sample was then desalted using Zip-Tip C18 pipette tips (Millipore, Billerica, MA, USA).

Nano-HPLC–MS/MS analysis was carried out using a Dionex Ultimate 3000 HPLC system equipped with an EASY-Spray™ capillary column (15 cm × 150 μm, 2 μm particle size, 100 Å pore size, C18). The column was coupled to a Q-Exactive Orbitrap mass spectrometer (Thermo Fisher Scientific, San Jose, CA, USA) (Tavares et al., 2011). Mobile phase A consisted of 0.1% formic acid in water, while mobile phase B was composed of 0.1% formic acid in 80% acetonitrile (*v/v*). The flow rate was maintained at 0.300 μL/min, and the column temperature was set to 35 °C.

The acquired raw files were subjected to data analysis using Proteome Discoverer software (version 1.4) (Capraro et al., 2013). The searches were performed against the Uniprot reference *C. sativa* proteome (updated in July 2024; 30194 sequences). The enzyme specificity was set as unspecific and methionine oxidation, asparagine/glutamine deamidation and N-term acetylation were set as variable modifications (Tavares et al., 2011). Only peptides with high confidence were included for positive identification. All peptides were searched in SATPdb, a database of structurally annotated therapeutic peptides (Singh et al., 2016), and in DFBP, a database of food-derived bioactive peptides (Qin et al., 2022).

To consider possible further proteolysis, the search was performed keeping a minimum sequence length of four amino acids and applying an "IF" nested function to a matrix which compared the sequence of each peptide found with the ones of the database (Micrososft Excel 2023, version 16.80). The mass spectrometry raw data have been deposited in the ProteomeXchange Consortium (http://proteomecentral.proteomexchange.org) via the PRiDE partner depository with the dataset PXD066443.

2.2.3. Evaluation of the effects of hempseed protein isolate on short-term viability of C2C12 cells cultured in a 2D system

2.2.3.1. Short term cell viability. The murine C2C12 skeletal muscle cell line (IZSLER, Brescia, Italy) was grown for 14-18 passages in 75 cm^2 flasks using complete growth medium. Completed growth medium consisted of high-glucose DMEM (Sigma-Aldrich, Milan, Italy) supplemented with 10% FBS (Immunological Sciences, Rome, Italy), 2 mM L-glutamine (Sigma-Aldrich, Milan, Italy) and 1% penicillin/streptomycin (Immunological Sciences, Rome, Italy). When 80-90% confluence was reached, cells were detached using 5 mL of trypsin-EDTA 1X (Immunological Sciences, Rome, Italy) and then counted using the trypan blue staining method (Sigma-Aldrich, Milan, Italy) and a Neubauer chamber.

After trypsinisation, cells were seeded in 96-well plates at a density of 1.5×10^5 cells/mL, using the same complete medium as described above. After 24 h of incubation at 37°C and 5% CO_2, necessary for cell adhesion and proliferation, the culture medium was removed and replaced with different decreasing concentration of HSPI (0.53-0.02 mg/mL). The cells were then incubated for a further 24 and 48 h. Cell viability was assessed using the Alamar Blue colorimetric kit (Immunological Sciences - Società Italiana Chimici, Rome, Italy). For the assay, 10 μL of ready-to-use reagent was added to each well containing 100 μL of culture medium. The plates were shaken for 30 s and then incubated for 2 h at 37°C in an atmosphere with 5% CO_2. At the end of the incubation, absorbance was read using a spectrophotometer at a wavelength of 570 nm. To correct for possible background interference, cell-free culture medium samples were read at 600 nm. Cell viability was calculated by subtracting the optical density (OD) value of the culture media (without cells) from the OD value at 570 nm obtained for the wells containing cells. The values thus obtained were normalised against the negative control (cells cultured in DMEM without FBS) and statistically compared to the positive control (cells cultured in complete growth medium).

2.2.3.2. Cell morphology. The HSPI concentration found to be most effective in supporting cell viability in 2D culture after 24 and 48 h was selected for analysis of cell morphology. The treatments evaluated were: 0.01 mg/L HSPI, 1% Insulin-Transferrin-Selenium supplement (ITS, Thermo Fisher Scientific S.p.A., Massachusetts, USA), 10% FBS and 0% FBS. The use of ITS was selected based on its chemically defined composition and its well-documented ability to actively support cell proliferation (Mainzer et al., 2014). Cell morphology was monitored throughout the proliferation phases (24 and 48 h) using an inverted light microscope with a 10 × objective lens (Optika, Bergamo, Italy). Four fields were analyzed for each treatment group, and the most representative images were included in the results. Before imaging, cells were rinsed with 1 × Phosphate-Buffered Saline (PBS).

2.2.3.3. RNA isolation and qRT-qPCR analysis. The experimental concentrations used for cell morphological evaluation at 24 and 48 h were selected to be subsequently used for gene expression analysis of key markers associated with cell proliferation. Particularly, total RNA was extracted from the C2C12 cells (1.5×10^5 cells/mL) cultured in 6-well plates using the GenElute™ Mammalian Total RNA Miniprep Kit (Sigma-Aldrich) following the manufacturer's instructions. RNA samples were quantified using a Nanodrop spectrophotometer (BioTek Synergy HTX Multimode Reader), normalized (~200 ng), and then reverse transcribed into cDNA using the SensiFAST cDNA Synthesis Kit (Meridian Bioscience). The temperature profile set in the thermal cycler (T100TM, Bio-Rad) for cDNA synthesis was as follows: 25°C for 10 min (annealing), 42°C for 15 min (reverse transcription), and 85°C for 5 min (inactivation). Subsequently, qPCR was performed with 1:4 diluted cDNA template in molecular-grade water, using the 2X SYBR Green Fast qPCR High ROX Mix (Fisher Molecular Biology) as per the manufacturer's instructions. PCR reactions were carried out on 7300 Real Time

PCR system (Applied Biosystems) with the thermal profile as follows: 95°C for 3 min (Initial denaturation), 95°C for 5 s (denaturation), 60°C for 31 s (annealing/extension), and repeated for 40 cycles with a melt curve. The relative expression levels of mRNA were calculated using the $2^{-\Delta\Delta Ct}$ method. Results were normalized to the expression levels of Glyceraldehyde-3-phosphate dehydrogenase (GAPDH) gene. All primer sequences are shown in Table 1.

2.2.4. Evaluation of the effects of hempseed protein isolate on long-term cell proliferation

To evaluate the long-term effects on C2C12 proliferation, cells were seeded in 100 × 20 mm Petri dishes (Falcon®, Corning Inc., Corning, NY, USA) at a density of 5×10^5 under four conditions: (i) 10% FBS, (ii) 2.5% FBS, (iii) 2.5% FBS supplemented with 0.01 mg/mL HSPI, and (iv) 2.5% FBS supplemented with 1% ITS. Cells were cultured for 6 days and passaged upon reaching approximately 70–80% confluence. At each passage, cells were stained with trypan blue and counted using a TC20 automated cell counter (Bio-Rad Laboratories, Inc., Hercules, CA, USA).

At the day six, 1×10^6 cells were collected and cryopreserved in standard freezing medium composed of 20% FBS, 10% dimethyl sulfoxide (DMSO), and 70% DMEM, as described by Baldeweg et al. (2025). Following two weeks of storage in liquid nitrogen, cells were thawed, and viability was assessed by trypan blue exclusion using the automated counter. Cells were subsequently reseed and maintained in culture for an additional 10 days with passaging performed whenever cultures reached approximately 70-80% confluence.

Cumulative proliferation was calculated separately for the pre-freezing and post-thaw periods as $\log_2$ fold change, spanning from day 0 to day 6 for the pre-freezing phase and day 0 (post-thaw) to day 10 for the post-thaw phase. This metric served as a comprehensive indicator of the proliferative capacity associated with each tratments across the full duration of the study.

2.2.4.1. Evaluation of intracellular protein levels and antioxidant activity at the end of long-term proliferation. At the end of the one-month proliferation period, cells were harvested and counted. An aliquot of 1×10^7 cells was collected by centrifugation at 1,500 rpm for 5 min. To investigate biochemical changes induced by the different culture conditions, cell lysis was performed according to a modified protocol based on Gioria et al. (2014). The cell pellet was resuspended in 1.5 mL of lysis buffer (20 mM Tris–HCl, pH 7.0; 100 mM NaCl; 1 mM EDTA; 0.5% Triton X-100) supplemented with 100 µL of protease inhibitor cocktail to prevent protein degradation and then subjected to sonication for 1 min. Complete lysis was verified microscopically. The lysates were centrifuged at 2,000 rpm for 2 min, and the resulting supernatants were collected for subsequent biochemical analyses.

Intracellular protein content was determined using the bicinchoninic acid (BCA) assay with the Pierce™ BCA Protein Assay Kit (Cat. No. 23225; Thermo Scientific), following the manufacturer's instructions with minor adaptations for small sample volumes. Samples and bovine serum albumin (BSA) standards at known concentrations were incubated with BCA working reagent for 30 min at 37°C. Under alkaline conditions, proteins reduce Cu^{2+} to Cu^{1+}, which subsequently forms a purple-colored complex with bicinchoninic acid. The absorbance of this complex, directly proportional to protein concentration, was measured at 562 nm using a Synergy™ 200 multi-mode microplate reader (Tecan Group Ltd.). Protein concentrations were calculated by interpolation from the BSA standard curve, with at least three technical replicates per sample. Values were normalized to the initial cell number (1×10^7 cells) and expressed as picograms (pg) per cell.

Antioxidant activity was evaluated using the 2,2-diphenyl-1-picrylhydrazyl (DPPH) assay, following the method described by Prieto et al. (2012), with slight modifications. The DPPH stock solution (0.2 mM) was prepared by dissolving 39.4 mg of DPPH (Merck KGaA) in methanol and adjusting the final volume to 500 mL in a calibrated volumetric flask. The solution was stored at 4°C in the dark until use. The assay was performed in 96-well microplates by adding 100 µL of DPPH solution and 100 µL of appropriately diluted sample to each well. Control wells contained either DPPH solution only (positive control) or solvent only (blank). Plates were incubated for 30 min at RT in the dark, and absorbance was measured at 517 nm using a microplate reader (Tecan Group Ltd.).

In addition to cell lysates, total protein content and antioxidant activity were also measured in the culture medium collected from each treatment condition.

2.2.5. Evaluation of the effect of hempseed protein isolate in 3D-bioprinting

As previously mentioned, HSPI in 3D was evaluated both as a supplement to the culture medium and as a functional component of the bioink used in the 3D-bioprinting process, as detailed in the following sections.

2.2.5.1. Alginate-Gelatin bioink formulation. Two stock solutions of gelatin and alginate were prepared for the formulation of the Alginate-Gelatin bioink (hereinafter referred as Alg-Gel bioink) (Zanderigo et al., 2023). The two stock solutions were prepared by dissolving Sodium Alginate powder and Gelatin powder in Milli-Q water to achieve a final concentration of 20% (*w/v*) for gelatin and 10% (*w/v*) for alginate. The two solutions were left under mechanical stirring for at least 6 h, at 50°C for alginate and at 40°C for gelatin, to achieve the powders' full hydration. Then, the desired amount of alginate stock solution was firstly loaded in a 3 mL syringe with Luer-Lock tip. The gelatin stock solution was heated at 37°C in water and loaded in a second 3 mL syringe with Luer-Lock tip. The alginate and gelatin solutions were then mixed at a mass ratio 3:1 (alginate to gelatin) by connecting the two syringes with a Luer-Lock. Then, a $CaCl_2$ 0.34 M solution was added to the ink in a mass ratio ink to $CaCl_2$ 8:1. Finally, prior bioprinting, the cell suspension was added to the bioink in a mass ratio 9:1 (ink to cell suspension), resulting in a final concentration of 6% *w/v* Alginate and 4% *w/v* Gelatin in the bioink. The cell suspension was prepared as follows: T_{75} flasks containing the 2D cells cultures were treated with Trypsin-EDTA (2 mL per T_{75} flask), pelleted by centrifugation (1200 rpm, 5 min) and removal of the supernatant, and finally suspended in basal medium (only DMEM) to achieve a final cell concentration of 7×10^6 cells/mL in the bioink.

2.2.5.2. Alginate-Gelatin with hempseed protein isolate bioink formulation. For the preparation of the Alginate-Gelatin bioink containing HSPI, two stock solutions were prepared. i) 20% (*w/v*) gelatin stock solution was prepared accordingly to the same protocol used for the Alg-Gel bioink. ii) A second stock solution was prepared by diluting HSPI solution with Milli-Q water until achieving a protein concentration of 0.0167 mg/mL. Sodium Alginate powder was then added to protein solution to achieve a final concentration of 10% (*w/v*) of alginate. The two stock solutions were then mixed as in a mass ratio 3:1 (alginate/HSPI to gelatin) using 3mL syringes as for the Alg-Gel bioink. Then, the $CaCl_2$ 0.34 M solution was added to the ink in a mass ratio ink to $CaCl_2$ 8:1. Finally, prior bioprinting, the cell suspension was added to the bioink in a mass ratio 9:1 (ink to cell suspension), resulting in a final concentration of 6% *w/v* Alginate, 4% *w/v* Gelatin and 0.01 mg/ml HSPI

Table 1
Forward (F) and reverse (R) primer sequences of Cyclin D1, CDK4 and GAPDH genes. CDK4: Cyclin-Dependent Kinase; GAPDH: Glyceraldehyde-3-phosphate dehydrogenase.

Gene	Primer sequences
Cyclin D1	F-TAGGCCCTCAGCCTCACTC
	R-CCACCCCTGGGATAAAGCAC
CDK4	F-AGTTTCTAAGCGGCCTGGAT
	R-AACTTCAGGAGCTCGGTACC
GAPDH	F-GTGTTCCTACCCCCAATGTG
	R-AGGAGACAACCTGGTCCTCA

in the bioink. Cell suspension was prepared using the same protocol adopted for the Alg-Gel bioink.

2.2.5.3. 3D-bioprinting. A BioX (Cellink, Langfilsgatan 7, 412 77 Gothenburg, Sweden) bioprinter was used for this work. The printer was equipped with the pneumatic extrusion print head containing the ink-loaded cartridge with a conical nozzle of 22G (0.410 mm). The printing process was performed at 37°C and 70 kPa, with a printing velocity of 20 mm/s. The printed scaffolds were designed using the software Autodesk Fusion 360 and consisted in two-layers grids, 10 by 10 mm side and 0.8 mm height. Each layer was characterized by a nominal thickness of 0.4 mm. After printing, the scaffolds were submerged in a 0.1 M $CaCl_2$ solution for 10 min to complete the physical crosslinking, then rinsed in PBS solution for 5 min to remove the excess of ions.

2.2.5.4. 3D cell viability and proliferation. Following the final PBS wash, the prepared constructs were treated and incubated under standard cell culture conditions (i.e., 37°C, 5% CO_2). One third of the prints was cultured under conventional culturing media composed of DMEM containing 10% FBS, 1% Glutamine and 1% Pen/Strep. The second third of the prints were cultured in a media composed of DMEM containing 0.01 g/ml of HSPI, 1% Glutamine and 1% Pen/Strep. The final third of the prints was instead cultured under DMEM alone containing only 1% Glutamine and 1% Pen/Strep. Every two days, for each of the condition, the media were replaced (after well washed)

The cell viability was evaluated using the Live/Dead (L/D) assay at three defined time points: immediately after printing (day 0), and on day 3 and day 7. Cells were stained with a solution of Calcein-AM (1.25 μM) and Ethidium Homodimer (4 μM) in sterile DMEM. At each investigated time point, three 3D-bioprinted constructs for each condition were washed in PBS and incubated with the staining solution for 1 h. Z-stack images of the stained cells were acquired using a confocal microscope (Fluoview FV10i, Olympus Life Science, England) equipped with an integrated incubator, four diode lasers (wavelengths: 405, 473, 559, and 635 nm), and a 10x phase-contrast objective (0.4 NA), producing images with a field of view of 1.2 × 1.2 mm^2. The pinhole size was set to 1 Airy Units. Live cells were imaged in the green channel (excitation 488 nm, emission 490-540 nm), dead cells in the red one (excitation 559 nm, emission 570-620 nm). Images were acquired at a resolution of 1024 × 1024 pixels, with a voxel size of 0.7 × 0.7 × 11 mm. The micrographs were analysed using the Image-J software to estimate the cell viability percentage, according to Equation 1:

$$Cell\ Viability\ [\%] = \frac{N_{live}}{N_{live} + N_{dead}} \cdot 100$$

Where N_{live} indicates the counted calcein-stained cells, and N_{dead} the counted ethidium-stained cells.

3. Statistical analysis

All data were analyzed using GraphPad Prism version 9.3.1 (GraphPad Software Inc., San Diego, CA, USA). The effects of HSPI on 2D cell viability at 24 and 48 h, on the expression of proliferation-related genes, and on long-term proliferation were assessed by one-way ANOVA followed by Tukey's multiple comparisons test. Cell viability in 3D after the bioprinting process was evaluated using an independent-samples t-test, assuming equal variances between groups. Data are presented as mean ± standard error of the mean (SEM) from at least three independent experiments. Statistical significance was set at $P \leq 0.05$ (95% confidence interval).

4. Results

4.1. Protein and peptidomic characterization and analysis of potential bioactive endogenous peptides

Hempseed protein isolate was analyzed by a shotgun label free MS analysis to characterize the proteomic and peptidomic profiles as described in the Methods section. This approach allowed the identification of 231 proteins and 500 endogenous peptides, as reported in Supplementary Table 1 and 2, respectively. All peptides found in HSPI (Supplementary Table 2) were searched in DFBP, a database of bioactive peptides of food origin, and in SATPdb, a database of structurally annotated therapeutic peptides. Table 2 lists the total number of bioactive peptides identified with high confidence level (Xcorr 1.5), categorized by their activity type while the list of the corresponding peptides is reported in Supplementary Table 3.

Analysis was performed on the proteins identified (Supplementary Table 1) to further characterize the HSPI proteome (Fig. 1a and 1b). The Gene Ontology Cellular Component (GOCC) analysis (Fig. 1A) revealed that a substantial proportion of proteins are localized in the cytosol (24%) or cytoplasm (33%), with over 18% identified as mitochondrial proteins. Additionally, a smaller fraction (3%) is associated with the intracellular anatomical structures of the cell. KEGG pathway analysis (Fig. 1b) demonstrated a significant enrichment in bioenergetic pathways (over 62%), followed by protein processing (12%) and cellular defence mechanisms, including glutathione metabolism (9%) and plant–pathogen interaction pathways (12%).

4.2. Evaluation of the effect of hempseed protein isolate on cell viability of C2C12 cells in 2D culture

The effects of HSPI on C2C12 cell viability, assessed by the Alamar Blue assay, are shown in Fig. 2a and 2b, after 24 and 48 h of treatment, respectively. Concentrations above 0.53 mg/mL were not included as they produced no detectable signals by the assay, indicating marked cytotoxicity. As shown in Fig. 2a, concentrations of 0.53 mg/mL (56.50 ± 13.30 %), 0.25 mg/mL (43.03 ± 19.66 %) and 0.2 mg/mL (60.06 ± 1.34 %) significantly reduced cell viability compared to the positive control (117.83 ± 3.69 %) after 24 h of incubation. The same trend was confirmed at 48 h (Fig. 2b). All other tested concentrations did not show any significant differences compared to the positive control (10% FBS). The highest absolute values were recorded at 0.01 mg/mL HSPI, reaching 110.10 ± 3.33% and 118.93 ± 2.66% at 24 and 48 h, respectively.

4.3. Evaluation of cell morphology

The morphological analysis of C2C12 cells cultured in 2D conditions is reported in Fig. 3.

Morphological analysis of the 2D cultured cells, conducted by phase-

Table 2
Total number of bioactive peptides identified with high confidence level (Xcorr 1.5), categorized by their activity. ACE: Angiotensin Converting Enzyme; DPP: dipeptidyl-peptidase.

	SATPdb (conf: HIGH, Xcorr 1.5; 500 peptides)	DFBP
TOTAL BIOACTIVE PEPTIDES	7	15
Antioxidant	/	2
ACE-inhibitor	2	5
Antibacterial	/	/
Antihypertensive	5	2
DPP IV-inhibitory	/	1
Immunomodulatory	/	1
PEP-inhibitory	/	1
Celiac disease	/	1

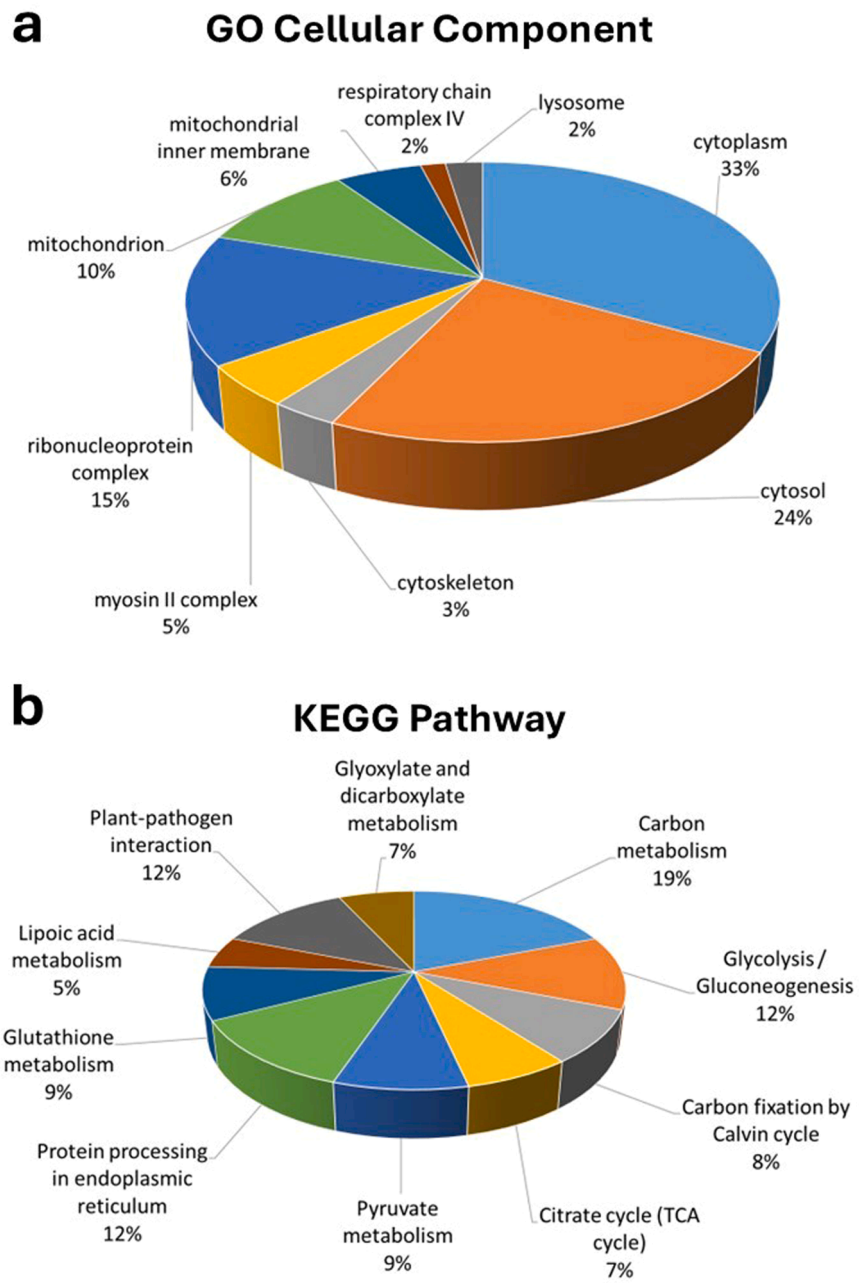

Fig. 1. Bioinformatic analysis of the proteins identified in hempseeds protein isolate. A) GOCC analysis by David software. B) KEGG pathway analysis. Functional grouping was based on Fischer's exact test ($P \leq 0.05$). GO: Gene Ontology; KEGG: Kyoto Encyclopedia of Genes and Genomes.

contrast microscopy at 24 and 48 h, revealed differences between the experimental conditions tested. In the absence of FBS, cells showed poor adhesion to the substrate and limited proliferation, maintaining an isolated and barely elongated morphology even after 48 h. In contrast, treatment with 10% FBS resulted in optimal adhesion, typical cell morphology and a progressive increase in cell density, indicative of high mitogenic activity. The HSPI supplement (0.01 mg/mL) sustained a good proliferative capacity, exhibiting a cell morphology comparable to FBS supplemented culture, and achieved significantly higher cell density than the negative control. This trend was also confirmed with 1% of ITS.

4.4. Molecular assessment of cell proliferation

Gene expression analysis at 48 h (Fig. 4) was performed to evaluate the transcriptional modulation of two cell proliferation markers, Cyclin D1 and Cyclin-Dependent Kinase 4 (CDK4), in response to the different culture conditions: HSPI (0.01 mg/mL), 1% ITS, and 10% FBS. Expression levels were normalized relative to the negative control (0% FBS, set as reference value of 1), enabling direct comparative analysis of the different treatments.

The gene expression results were consistent with the morphological observations, showing no statistically significant differences between the treatments and the positive control (10% FBS).

4.5. Evaluation of the effect of hempseeds protein isolate on long term proliferation

Fig. 5 presents the results of the long-term proliferation. All experimental conditions were conducted in the presence of 2.5% FBS, as the treatments alone were insufficient to support cell adhesion. Lower serum levels (~1%) were avoided because they may induce morphological alterations in C2C12 cells (Milesi et al., 2024). As shown in

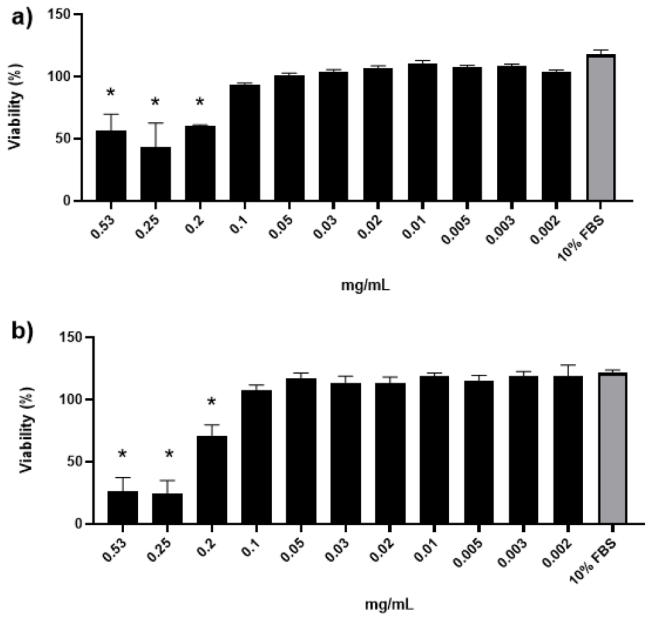

Fig. 2. Cell viability (%) of C2C12 cells treated with hempseeds protein isolate (HSPI) assessed with the Alamar Blue assay. a) 24 h of treatment; b) 48 h of treatment. Values, expressed in %, are represented as mean ± SEM. Values are standardised on growth medium (0% FBS) and expressed in mg/mL. * indicates statistically significant differences ($P \leq 0.05$) compared to positive control (10% FBS).

Supplementary Fig. 1, 2.5% FBS significantly ($P \leq 0.05$) reduced cell viability at 48 h, thereby providing a more sensitive experimental context for evaluating HSPI-mediated effects.

Cell proliferation, expressed as log2(fold change) over the first 6 days prior to cryopreservation (Fig. 5a), did not show significant differences among all groups. A comparable trend, albeit without statistically significant differences, was observed in post-thaw cell viability (Fig. 5b) and during the subsequent 10 days of proliferation (Fig. 5c).

Significant findings emerged from the analysis of intracellular protein content and intracellular antioxidant activity at the end of the complete proliferation period. As shown in Fig. 5d, although culture media supplemented with 2.5% FBS were characterized by a significantly ($P \leq 0.05$) lower protein content compared to 10% FBS, no statistically significant differences were observed in intracellular protein levels among all the experimental groups.

Conversely, an opposite trend was observed for antioxidant activity. As reported in Fig. 5e, supplementation of the culture medium with HSPI significantly ($P \leq 0.05$) enhanced the antioxidant profile, showing statistically significant differences ($P \leq 0.05$) compared with other treatments. These differences were partially reflected at the intracellular level. Specifically, intracellular antioxidant activity was significantly higher ($P \leq 0.05$) in the 2.5% FBS + HSPI and 2.5% FBS + 1% ITS groups compared with 2.5% FBS and 10% FBS conditions ($P < 0.05$).

4.6. Evaluation of the effect of hempseeds protein isolate in 3D-bioprinting

To evaluate the potential of HSPI as a functional ingredient for 3D skeletal muscle tissue models, bioprinted constructs were developed with HSPI incorporated either into the culture medium, into the bioink formulation, or in both. This experimental design aimed to compare the effects of HSPI as a medium supplement versus direct hydrogel incorporation, enabling independent and combined assessment of the two delivery methods. Six experimental conditions were defined (Fig. 6).

In the first group, constructs were printed using a conventional alginate-gelatin bioink and subsequently cultured under three conditions: (i) DMEM without supplementation (negative control), (ii) DMEM supplemented with 10% FBS (positive control), and (iii) DMEM supplemented with 0.01 mg/mL HSPI. In the second group, constructs were printed with the same bioink, enriched with 0.01 mg/mL HSPI, and cultured under the same three conditions to allow parallel comparisons. Cell viability was assessed at days 0, 3, and 7 using L/D staining, and values were expressed as normalized L/D ratios relative to the negative

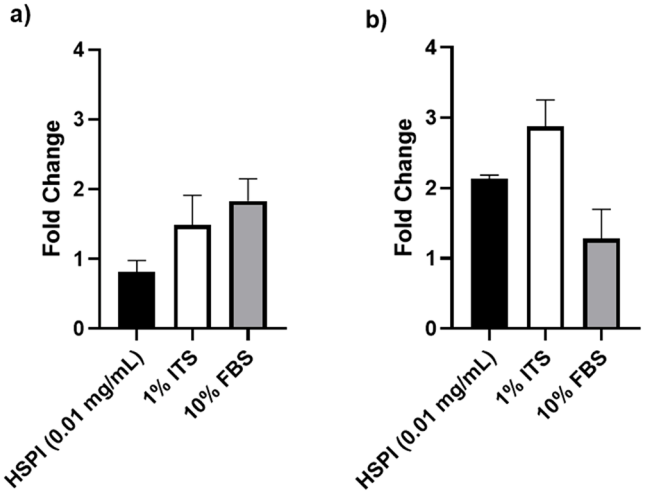

Fig. 4. Gene expression of Cyclin D1(a) and Cyclin-Dependent Kinase 4 (b) in C2C12 cells after 48 h of treatment. Results are expressed as fold-change relative to the negative control (0% FBS) and presented as mean ± SEM. FBS: Fetal Bovine Serum; HSPI: Hempseed Protein Isolate; ITS: Insulin-Transferrin-Selenium.

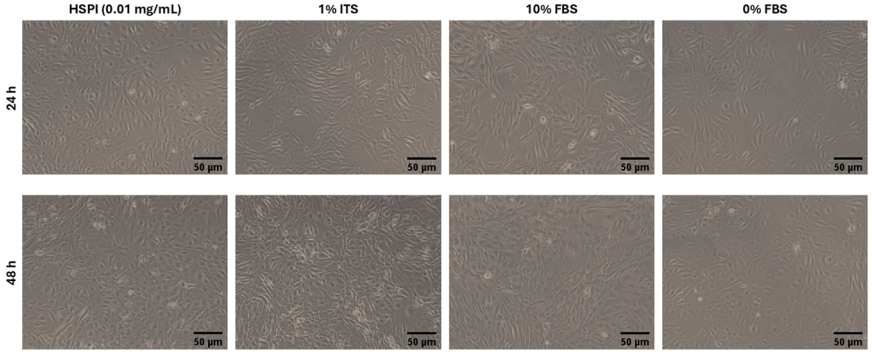

Fig. 3. Morphology of C2C12 cells cultured in media supplemented with HSPI (0.01 mg/mL), 1% ITS, 10% FBS and 0% FBS. 24 h and 48 h correspond to the cell proliferation stage with or without FBS, HSPI or ITS. Images were acquired at 10 × magnification. FBS: Fetal Bovine Serum; HSPI: Hempseeds Protein Isolate, ITS: Insulin-Transferrin-Selenium.

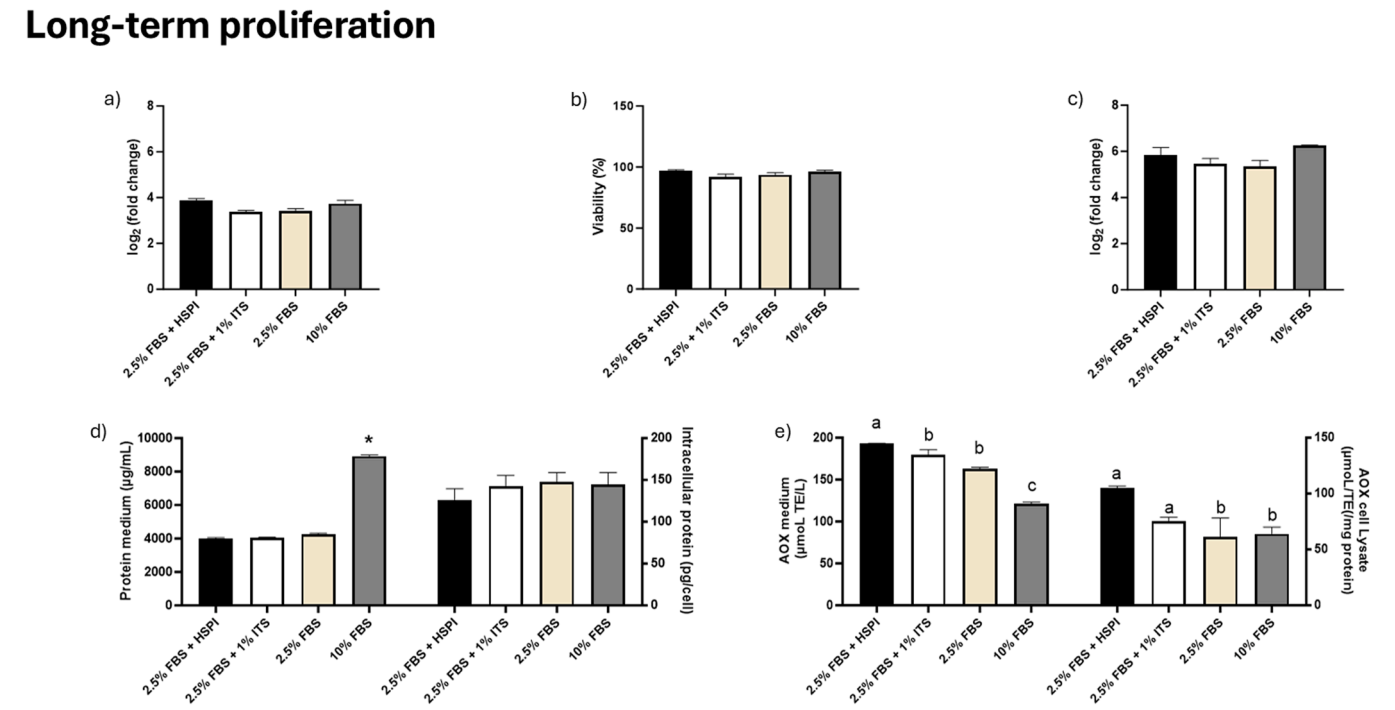

Fig. 5. Long term proliferation. (a) Cell proliferation from Day 0 to Day 6 prior to cryopreservation. Results are expressed as mean ± SEM of log2(fold change). * Indicates statistically significant differences ($P \leq 0.05$). (b) Cell viability following cryopreservation. Results are expressed as percentage (%) mean ± SEM. (c) Cell proliferation from Day 0 to Day 10 after thawing. Results are expressed as mean ± SEM of log2(fold change). (d) Protein content of the cell culture medium and intracellular protein content. Results are expressed as mean ± SEM. Protein concentration in the cell culture medium is reported as µg/mL, while intracellular protein content is expressed as pg/cell. * indicates statistically significant differences ($P \leq 0.05$). (e) Antioxidant activity of the culture medium and intracellular antioxidant activity. Results are expressed as mean ± SEM. Antioxidant activity in the culture medium is expressed as µmol Trolox equivalents (TE)/mL, whereas intracellular antioxidant activity is expressed as µmol TE/mg protein. Different letters indicate statistically significant differences ($P \leq 0.05$).

control.

At day 0, constructs printed with conventional bioink showed L/D ratios of 98% (HSPI) and 101% (FBS), while constructs printed with enriched bioink showed values of 100% (HSPI) and 97% (FBS), with no significant differences among groups. At day 3, a general increase in cell viability was observed: constructs with conventional bioink reached 226% (HSPI) and 196% (FBS), whereas those with enriched bioink reached 180% (HSPI) and 193% (FBS), indicating active cell proliferation under all supplemented conditions. At day 7, viability remained high: 182% (HSPI) and 228% (FBS) for the conventional bioink, and 182% (HSPI) and 209% (FBS) for the enriched bioink. Statistical analysis revealed no significant differences in cell viability between HSPI- and FBS-treated samples across all time points and conditions, except for constructs printed with conventional bioink at day 7, where a significant difference was observed between supplemented and unsupplemented groups ($P < 0.05$).

5. Discussion

The growing interest in CM has prompted the scientific community to investigate its opportunities and challenges as a rapidly evolving biotechnological field.

One of the major challenges in cellular agriculture today is the reliance on culture media containing FBS, a complex and undefined component of animal origin (Sundaram et al., 2025). While significant progress has been made in developing serum-free media formulations, their high cost and limited scalability still represent major obstacles for the large-scale and economically viable production of CM (Dolgin et al., 2025).

To address this, recent research has increasingly focused on identifying plant-based alternatives, particularly food industry co-products, that align with sustainability principles and the ethical values at the core of this field (Stout et al., 2023).

In this context, hemp-based products stand out due to their low environmental impact and rich nutritional and functional profile, making them a promising alternative (Farinon et al., 2020). Nevertheless, their potential remains largely unexplored in the field of cell feeding.

Peptidomic analysis allowed the identification of 231 proteins and 500 endogenous peptides in HSPI, including numerous peptides with known or potential activity, highlights the biochemical complexity and multifunctional potential of HSPI (Farinon et al., 2020). Unlike traditional protein sources, which act primarily as nutritional substrates, HSPI offers a composite mixture of structural, metabolic and signalling components. The identification of antioxidant, angiotensin converting enzyme (ACE) inhibitor and antihypertensive peptides aligns with previous research underscoring the nutraceutical profile of HSs (Aguchem et al., 2022). Notably, this study represents an innovative contribution in that it suggests, for the first time to our knowledge, the potential of HSs to influence cellular behaviour *in vitro*, particularly in skeletal myoblasts.

The enrichment of KEGG metabolic pathways associated with bioenergetics, protein processing, and redox homeostasis, including glutathione metabolism, provides a contextual framework based on known biological functions. These pathways are well known for their role in supporting cell viability, proliferation, and stress management in skeletal muscle cells, which are highly dependent on mitochondrial ATP production and redox balance (Glancy and Balaban, 2021), especially under in vitro conditions where oxidative stress can be exacerbated (Halliwell, 2003).

The identification of HSPI components linked in the literature to glutathione turnover, chaperone activity, and energy metabolism is therefore compatible with, although not demonstrative of, possible influences on oxidative balance, protein folding, or metabolic stability

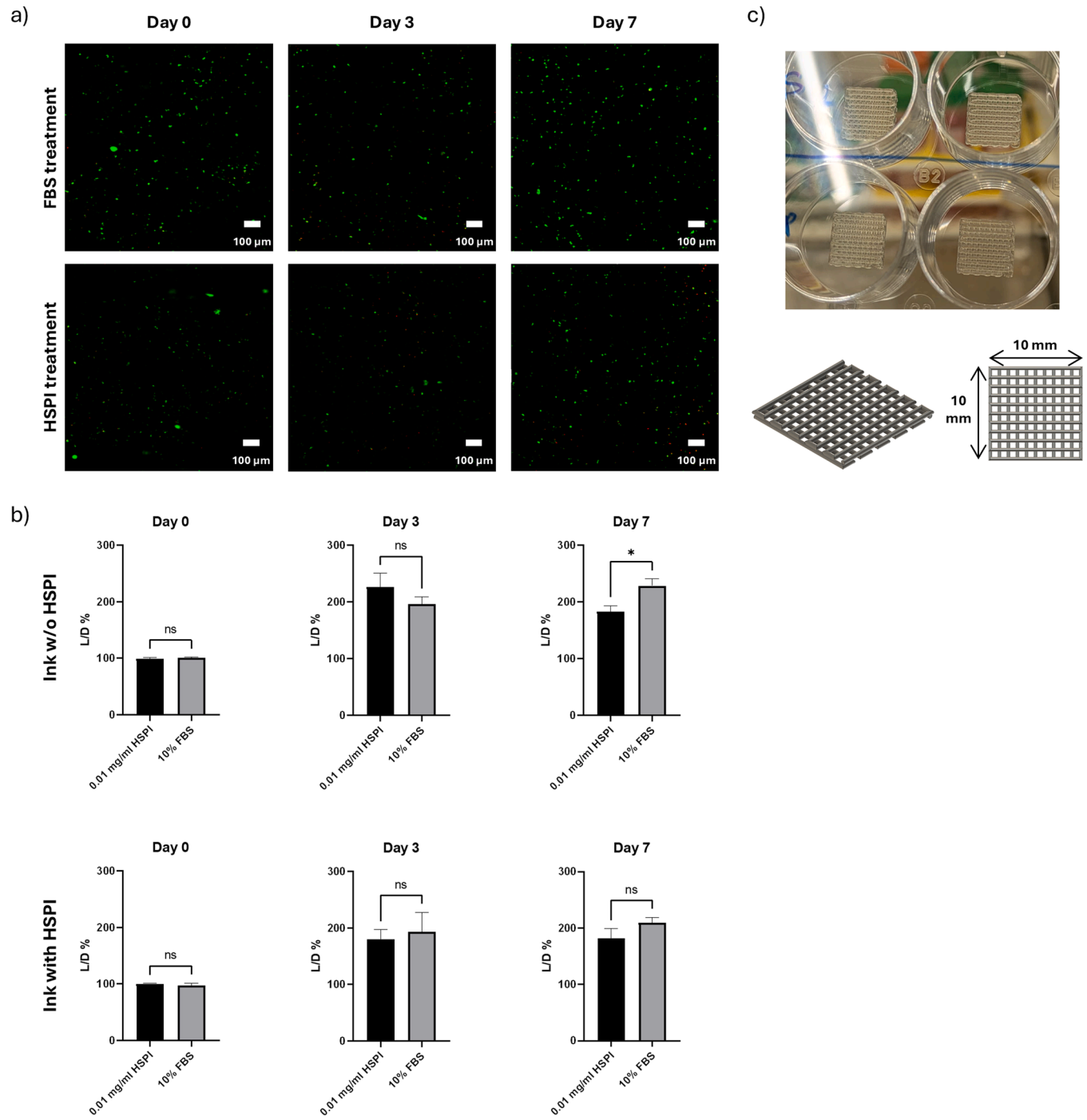

Fig. 6. a) Representative fluorescent live/dead (L/D) images of constructs treated with FBS or hemp extract at day 0, 3, and 7. Scale bar: 100 µm; b) Quantification of cell viability from L/D assays, expressed as relative viability compared to a negative control (constructs cultured in pure DMEM), for constructs printed with or without hemp. * Indicated statistically significant differences ($P < 0.05$); c) Computer-aided design (CAD) models and corresponding bioprinted constructs (geometry: 10 × 10 × 0.8 mm).

(Liang and MacRae, 1997). These considerations are intended as biologically plausible interpretations and require further investigation. Similarly, the presence of peptides previously reported for their ACE inhibitory activity may suggest potential interactions with the renin-angiotensin system, which exerts autocrine and paracrine effects in skeletal muscle. Given that angiotensin can promote ROS production (Sachse and Wolf, 2007), impair mitochondrial function (Mitsuishi et al., 2009), and reduce myoblast proliferation (Yoshida et al., 2013), ACE-inhibiting peptides could hypothetically attenuate these processes. However, this interpretation remains strictly inferential and is presented to frame possible mechanistic pathways rather than to assert functional evidence.

Overall, these notes reflect established biological functions reported in the literature and are offered as hypothesis-generating interpretations that may help guide future mechanistic studies.

These observations were confirmed by 2D-cell culture assays using C2C12 cell line. This cell line is widely used in laboratories due to its high reliability and ease of handling, representing an established model for the study of muscle differentiation. C2C12 is particularly useful in CM research, as it allows the proliferation and differentiation processes

of myoblasts to be investigated under controlled conditions, providing preliminary data that is fundamental for optimising cell growth and muscle tissue quality *in vitro* (Sundaram et al., 2025; Liu et al., 2025). The data obtained demonstrated a biphasic dose-response relationship to HSPI treatment. Specifically, lower concentrations promoted cell viability, whereas higher concentrations induced cytotoxic effects. This biphasic response aligns with the *hormesis paradigm*, characterized by stimulatory effects at subtoxic doses and inhibitory or toxic outcomes at elevated concentrations (Mattson, 2008). This principle is widely documented in the dose-response evaluation of bioactive compounds of food origin (Hayes, 2007; Jodynis-Liebert and Kujawska, 2020). Therefore, this study suggests that higher concentrations of HSPI may exert pro-oxidant effects, inducing ROS accumulation and resulting in decreased cell viability, as observed at both 24 and 48 h.

One of the main limitations of using high concentrations of proteins and peptides in cell culture media is osmotic stress: excessive protein solutes concentration increases medium tonicity beyond physiologically tolerable limits, thereby adversely affecting mammalian cell viability and proliferation (Beck et al., 2000). In addition, the possible accumulation of specific metabolites—such as free aromatic amino acids or polyphenol-bound peptides—may exert cytostatic or cytotoxic effects, depending on their concentration and the physiological state of the cells (Nikawa et al., 2021).

The morphological evaluation further confirmed the observations described above: at low concentrations (0.01 mg/mL), HSPI effectively supported cell proliferation, showing behaviour comparable to that observed with 10% FBS. This represents a significant result, albeit limited to the short term (up to 48 h). It is well known that FBS is the gold standard in cell culture (Van der Valk et al., 2018), thanks to its ability to provide an environment rich in growth factors, promote rapid adhesion and support high cell proliferation (Lee et al., 2022) At the same time, C2C12 cells cultured in the presence of 1% ITS allows further evaluation of the proliferative potential of HSPI in a defined and controlled environment. ITS is a mixture of three functional components: insulin which acts as a growth factor, stimulating nutrient uptake and the activation of mitogenic pathways; transferrin that provides bioavailable iron, essential for DNA synthesis and mitochondrial function and selenium, a cofactor of antioxidant enzymes such as glutathione peroxidase, contributing to the control of oxidative stress and redox balance (Straus, 1981; Karlenius et al., 2011; Ahmad et al., 2023). Although ITS lacks the full complexity of FBS, it is a valuable tool for assessing the efficacy of individual ingredients. The fact that HSPI achieved morphological results similar to ITS suggests that it is capable of providing these factors essential for cell proliferation, an aspect that was also confirmed when the two ingredients were used in combination.

At the same time, the analysis of Cyclin D1 and CDK4 expression indicates that HSPI supports cell survival and may be compatible with a modest enhancement of cell cycle activity, particularly at the G1–S transition. Cyclin D1, synthesised early in response to mitogenic cues, forms a complex with CDK4 that contributes to the phosphorylation of the retinoblastoma protein and to the subsequent release of E2F transcription factors required for S-phase entry (Stacey, 2003). The expression levels observed in HSPI-treated cells, comparable to those in FBS-supplemented conditions, suggest a possible alignment with established regulatory mechanisms governing cell cycle progression, although no direct mechanistic conclusions can be drawn.

These results may also reflect the nutritional composition of HSPI, which includes amino acids such as arginine, glutamine and branched-chain amino acids, known in the literature to participate in pathways associated with cellular growth and metabolism (Neinast et al., 2019). Similarly, the detection of peptides previously described as having antioxidant properties could be consistent with, rather than indicative of, a potential contribution to maintaining redox balance (Zhu et al., 2024). Overall, these interpretations should be viewed as cautious, hypothesis-generating considerations, grounded in known biological functions and not intended to imply direct mechanistic effects of HSPI. Further studies would be required to clarify the extent to which these components may influence the observed cellular responses.

The absence of statistically significant differences in expression levels between the HSPI+ITS, ITS alone and FBS groups confirms the robustness of the pro-proliferative effect of HSPI. To gain a more comprehensive understanding of the isolate's effects on myoblast biology, it would be valuable to expand the molecular analysis to incorporate markers of G2/M phase progression and mitotic regulators.

Certainly, in the field of cellular agriculture, it is essential to identify alternatives to animal origin ingredients capable not only of sustaining cell viability in the short term, but also of ensuring stable and lasting proliferation in the long term. For this reason, in the present study, cells were maintained in culture for a total duration of one month, including a two-week cryopreservation phase, to better simulate realistic operating conditions.

However, as previously reported, it was necessary to include a low percentage of FBS in the treatments, as complete serum deprivation prevented adequate cell adhesion to the culture surface (Fig. 5). This underscores the challenges of effectively replacing FBS, which supplies not only essential growth factors for proliferation, but also a complex set of components critic for adhesion, survival and maintenance of cellular homeostasis (Van der Valk et al., 2018).

The results in Fig. 5 highlight that HSPI supplementation in the presence of 2.5% FBS sustains a proliferative capacity comparable to both the 2.5% FBS condition and the control 10% FBS control, during both the pre-cryopreservation phase and after post-thaw recovery. This indicates that the isolate is biologically compatible with multiple replication cycles and does not induce cumulative cytotoxic or cytostatic effects. However, these results contrast with our previous study (Lanzoni et al., 2026), in which hydrolyzed hempseeds reduced cell viability and proliferation and induced morphological changes after 72 h. This discrepancy suggests that the extraction methods and treatment protocols applied to the matrices can substantially influence their cellular effects (Ghenabzia et al., 2023).

A key aspect of culture medium management concerned the ability to modulate both its nutritional and functional profiles. For this reason, the protein content of the medium was evaluated. The analysis confirmed that reducing the serum from 10% to 2.5% FBS resulted in a significant decrease in total protein concentration, while adding HSPI at the concentration used (0.01 mg/mL) did not quantitatively restore protein levels of 10% FBS. This indicated that the observed effect was not due to a simple increase in protein quantity, but rather to a qualitative contribution of the plant protein fraction. Consistent with these results, the intracellular protein content per cell showed no significant differences between the 2.5% FBS, 2.5% FBS + HSPI, 2.5% FBS + ITS, and 10% FBS conditions, suggesting that neither serum reduction nor HSPI supplementation altered the overall anabolic balance or cellular proteostasis.

The most distinctive aspect concerned antioxidant activity: the presence of HSPI led to a significant increase in the antioxidant capacity of the medium compared to both 2.5% and 10% FBS, with a partially detectable effect also at the intracellular level. This result is consistent with that observed by Lanzoni et al. (2026), where the inclusion of HSPI increased antioxidant activity. Considering that *in vitro* systems are characterised by oxygen tensions higher than physiological ones and a greater predisposition to oxidative stress (Jagannathan et al., 2016), the observed increase suggests a modulation of the extracellular redox microenvironment. This effect can plausibly be attributed to the presence of bioactive peptides with potential scavenger activity or to the availability of amino acids capable of indirectly supporting cellular antioxidant systems, in accordance with the data reported in Table 2.

Unlike ITS, whose effect can be attributed to selenium and the resulting activation of selenoenzymes such as glutathione peroxidase (Karlenius et al., 2011), the mechanism of HSPI appears less well-defined, likely acting by stabilizing the oxidative environment rather than directly promoting proliferation. The observation that the

increased antioxidant activity did not lead to higher proliferation compared with 2.5% FBS suggests that, under the experimental conditions used, the redox state was not a limiting factor for growth. Nevertheless, the modulation of antioxidant activity may contribute to long-term metabolic stability, supporting cellular resilience during extended expansion and cryopreservation. The increase in the antioxidant profile observed in the cell lysate at the end of the month culture period is particularly important, as one potential application of cultivated products is the ability to tailor their nutritional and functional profiles for specific consumer groups (Broucke et al., 2023).

Overall, the data suggest that HSPI, although not replacing serum mitogenic factors, can act as a functional component capable of integrating into formulations with reduced serum content, contributing to the biochemical and redox stability of the culture without altering its proliferative dynamics.

The assessment of cell viability in the bioprinted constructs made it possible to monitor the proliferative dynamics of C2C12 cells in a 3D context closer to the physiological environment, avoiding the use of FBS to promote adhesion. At day 0, i.e. immediately after bioprinting, all groups supplemented with FBS or HSPI - both in the medium and in the bioink - showed comparable levels of viability close to 100%, confirming that neither the printing process nor the composition of the bioinks, including the presence of HSPI, compromised initial cell survival. Nevertheless, as reported by Bomkamp et al. (2022), bioprinting exposes cells to mechanical stress, particularly to the shear forces generated during extrusion, which can compromise cell viability and delay cell proliferation.

At day 3, a general increase in cell viability was observed across all supplemented constructs, indicating active cell proliferation. Notably, HSPI-treated constructs exhibited a viability increase comparable to that observed with FBS, both when the supplement was added to the culture medium and when incorporated into the hydrogel matrix. This suggests that HSPI effectively support cell proliferation even under 3D conditions, regardless of the mode of administration, confirming the results of 2D. The most interesting difference emerges at day 7, a critical point in assessing the system's ability to maintain cell viability and activity over time. In conventional bioink constructs, cell viability of HSPI-treated groups in the medium was significantly reduced compared to FBS ($P < 0.05$), indicating a sustained decline in viability over time. However, incorporating HSPI into the bioink eliminates this difference: cell viability remains comparable to FBS levels, indicating, most probably, gradual and prolonged release of bioactive components from the matrix itself, a critical strategy for CM production (Levi et al., 2022). This observation supports the hypothesis that incorporating HSPI into the hydrogel matrix acts as a bioactive reservoir, enabling the controlled release of nutrients, amino acids, and bioactive peptides over time. Compared to direct supplementation in the culture medium, this strategy enhances energy metabolism and sustains cell proliferation while reducing the risks of rapid nutrient depletion and the accumulation of metabolic byproducts typically associated with direct medium supplementation.

From a bioengineering perspective, the absence of statistical differences in cell viability across all conditions on day 0 of the L/D assay suggests that the addition of HSPI did not introduce major adverse effects on the printing process or on the initial construct integrity. While cell viability is only an indirect indicator and cannot be used to conclusively infer rheological behaviour, this observation is consistent with the expected limited impact of HSPI on the alginate–gelatin matrix at the low concentration tested (0.01 mg/mL). This interpretation aligns with the chemical characteristics of the isolate: HSPI is primarily composed of edestin (Farinon et al., 2020), a low-grade gelling globulin that does not significantly influence the viscosity or cross-linking, particularly at the low concentrations (0.01 mg/mL) used in this study. Furthermore, the isolation process effectively removes insoluble fibres and polysaccharides, minimizing potential interference with the bioink's structure (Stout et al., 2023). The edestin, which lacks adhesive motifs or highly charged groups, does not compete with alginate for ionic cross-linking with Ca^{2+}, preserving the physical stability and printability of the system. Although direct rheological measurements would be required to fully confirm this, the available evidence indicates that HSPI is unlikely to substantially disturb the physical behaviour of the alginate–gelatin system under the conditions tested.

Overall, our data indicate that HSPI sustains cell viability in short-term 2D cultures (up to 48 h) and in 3D systems, particularly when incorporated into the matrix, while also contributing to the enrichment of the antioxidant profile of the culture system. However, this effect did not translate into enhanced long-term cell proliferation. This dual functionality, nutritional/functional support and redox modulation, positions HSPI as a strategic ingredient for the design of advanced bioinks aimed at the sustainable reduction of animal-derived components, such as FBS, in CM applications.

In light of these findings, alternative protein sources, particularly plant-derived ones, represent a key resource for progressively replacing animal-derived supplements in cell culture systems. This transition has direct implications for the development of more ethical, scalable, and economically viable production models aligned with the principles of cellular agriculture (Ho et al., 2021).

Despite the promising nutritional and functional profile of hemp-derived ingredients, their large-scale production remains limited, especially within the European context (Horne, 2020; Ely and Fike, 2022). Furthermore, the lack of a harmonised regulatory framework and the presence of legislative barriers—recently highlighted in Italy by Decree Law No. 48/2025, which introduces restrictions on hemp-based products in food and processed goods—represent concrete obstacles to the industrial development of hemp-derived ingredients (Federcanapa, 2025).

Nevertheless, within the CM sector, the availability of scalable, technically compatible, and cost-effective plant-derived functional ingredients is a crucial prerequisite for ensuring economic competitiveness (Ho et al., 2021). From this perspective, hemp emerges as a strategic and still underexploited agro-industrial resource whose full potential warrants further investigation at both scientific and regulatory levels. The present study represents an initial step toward the integration of hemp-derived components as functional ingredients in CM culture systems, highlighting their potential to contribute not only to medium formulation but also to the functional enhancement of cell-based products.

The authors acknowledge certain limitations, particularly those associated with the use of a specific cell line as the experimental model, which may partially constrain the generalizability of the findings. Nevertheless, this model may retain practical relevance in emerging and rapidly expanding sectors, including CM applications for the pet food market (Choudhury et al., 2020). Future studies should include additional cell lines, derived from different species and tissue types relevant to CM production, in order to further confirm the reproducibility and robustness of the observed effects. Extending validation across diverse cellular models, culture conditions, and longer-term production settings will be important to strengthen the translational potential of hemp-derived ingredients within next-generation cell-based food systems.

Ethics approval

Not applicable.

Financial support statement

The authors also acknowledge financial support under the National Recovery and Resilience Plan (NRRP), Mission 4, Component 2, Investment 1.1, Call for tender No. 104, published on 2.2.2022 by the Italian Ministry of University and Research (MUR), funded by the European Union – NextGenerationEU – Project Title "Cellular agriculture

for sustainable and innovative food production (CELLtoFOOD)" – CUP G53D23003940006 – Grant Assignment Decree No. 1048 adopted on 7.14.2023 by the Italian Ministry of Ministry of University and Research (MUR). The study was partly supported by the EU Joint Research Centre Exploratory Research programme ('ER-PT-2024-SUPERFOOD) and through the Portfolio "PF11 - Strategic technologies for economic security & innovative industrial ecosystems.

CRediT authorship contribution statement

D. Lanzoni: Writing – review & editing, Writing – original draft, Visualization, Validation, Software, Methodology, Investigation, Formal analysis, Data curation, Conceptualization. **G. Zanderigo:** Writing – review & editing, Writing – original draft, Visualization, Validation, Software, Methodology, Investigation, Formal analysis, Data curation, Conceptualization. **S. Nonnis:** Writing – review & editing, Visualization, Validation, Software, Methodology, Investigation, Formal analysis, Data curation. **G. Tedeschi:** Writing – review & editing, Writing – original draft, Visualization, Validation, Software, Methodology, Investigation, Formal analysis. **B.M. Colosimo:** Writing – review & editing, Visualization, Validation, Methodology, Investigation, Conceptualization. **S. Gioria:** Writing – review & editing, Visualization, Validation, Funding acquisition. **T.S. Sundaram:** Writing – review & editing, Visualization, Validation, Methodology, Data curation. **P.A. Corsetto:** Writing – review & editing, Methodology. **F. Cheli:** Writing – review & editing, Visualization, Validation. **C. Giromini:** Writing – review & editing, Writing – original draft, Visualization, Validation, Software, Project administration, Methodology, Investigation, Funding acquisition, Formal analysis, Data curation, Conceptualization.

Declaration of competing interest

The authors declare that they have no known competing financial interests or personal relationships that could have appeared to influence the work reported in this paper.

Acknowledgements

The authors would like to express their gratitude to the Department of Microbiology, Nutrition and Dietetics, Faculty of Agrobiology, Food and Natural Resources, Czech University of Life Sciences Prague (Kamycka 129, 165 00 Prague, Czech Republic) and the Department of Nutritional Physiology and Animal Product Quality, Institute of Animal Sciences (Pratelstvi 815, 104 00 Prague, Czech Republic) for their generous donation of the hempseeds (*Cannabis sativa* L., variety Futura) used in the present study.

Supplementary materials

Supplementary material associated with this article can be found, in the online version, at doi:10.1016/j.fufo.2026.101098.

Data availability

Data will be made available on request.

References

Addis, M.F., Maffioli, E.M., Ceciliani, F., Tedeschi, G., Zamarian, V., Tangorra, F., Bronzo, V., 2020. Influence of subclinical mastitis and intramammary infection by coagulase-negative staphylococci on the cow milk peptidome. J. Proteom. 226, 103885. https://doi.org/10.1016/j.jprot.2020.103885.

Aguchem, R.N., Okagu, I.U., Okagu, O.D., Ndefo, J.C., Udenigwe, C.C., 2022. A review on the techno-functional, biological, and health-promoting properties of hempseed-derived proteins and peptides. J. Food Biochem. 46 (7), e14127. https://doi.org/10.1111/jfbc.14127.

Ahmad, S.S., Chun, H.J., Ahmad, K., Shaikh, S., Lim, J.H., Ali, S., Choi, I., 2023. The roles of growth factors and hormones in the regulation of muscle satellite cells for cultured meat production. J. Anim. Sci. Technol. 65 (1), 16. https://doi.org/10.5187/jast.2022.e114.

Aletti, F., Maffioli, E., Negri, A., Santamaria, M.H., DeLano, F.A., Kistler, E.B., Tedeschi, G., 2016. Peptidomic analysis of rat plasma: proteolysis in hemorrhagic shock. Shock 45 (5), 540–554. https://doi.org/10.1097/SHK.0000000000000532.

Baldeweg, T.H., Hubel, P., Günther, J., Ostertag, F., Nellinger, S., Heine, S., Kluger, P.J., 2025. Dairy byproducts as sustainable alternatives to FCS in 2D and 3D skeletal muscle cell cultures. Bioresour. Bioprocess. 12 (1), 101. https://doi.org/10.1186/s40643-025-00938-w.

Bauzá-Martinez, J., Aletti, F., Pinto, B.B., Ribas, V., Odena, M.A., Díaz, R., de Oliveira, E., 2018. Proteolysis in septic shock patients: plasma peptidomic patterns are associated with mortality. Br. J. Anaesth. 121 (5), 1065–1074. https://doi.org/10.1016/j.bja.2018.05.072.

Beck, F.X., Grünbein, R., Lugmayr, K., Neuhofer, W., 2000. Heat shock proteins and the cellular response to osmotic stress. Cell. Physiol. Biochem. 10 (5-6), 303–306. https://doi.org/10.1159/000016362.

Benton, T.G., Bieg, C., Harwatt, H., Pudasaini, R., Wellesley, L., 2021. Food system impacts on biodiversity loss. Three levers for food system transformation in support of nature. Chatham House, London, pp. 02–03.

Bomkamp, C., Skaalure, S.C., Fernando, G.F., Ben-Arye, T., Swartz, E.W., Specht, E.A., 2022. Scaffolding biomaterials for 3D cultivated meat: prospects and challenges. Adv. Sci. 9 (3), 2102908. https://doi.org/10.1002/advs.202102908.

Broucke, K., Van Pamel, E., Van Coillie, E., Herman, L., Van Royen, G., 2023. Cultured meat and challenges ahead: A review on nutritional, technofunctional and sensorial properties, safety and legislation. Meat Sci 195, 109006. https://doi.org/10.1016/j.meatsci.2022.109006.

Capraro, J., Magni, C., Faoro, F., Maffi, D., Scarafoni, A., Tedeschi, G., Duranti, M., 2013. Internalisation and multiple phosphorylation of γ-conglutin, the lupin seed glycaemia-lowering protein, in HepG2 cells. Biochem. Biophys. Res. Commun. 437 (4), 648–652. https://doi.org/10.1016/j.bbrc.2013.07.026.

Chelladurai, K.S., Christyraj, J.D.S., Rajagopalan, K., Yesudhason, B.V., Venkatachalam, S., Mohan, M., Christyraj, J.R.S.S., 2021. Alternative to FBS in animal cell culture-an overview and future perspective. Heliyon 7 (8).

Choudhury, D., Tseng, T.W., Swartz, E., 2020. The business of cultured meat. Trends Biotechnol 38 (6), 573–577. https://doi.org/10.1016/j.tibtech.2020.02.012.

Dolgin, J., Chakravarty, D., Sullivan, S.F., Cai, Y., Lim, T., Yamaguchi, P., Nair, N.U., 2025. Microbial lysates as low-cost serum replacements in cellular agriculture media formulation. Food Res. Int. 201, 115633. https://doi.org/10.1016/j.foodres.2024.115633.

Eibl, R., Senn, Y., Gubser, G., Jossen, V., Van Den Bos, C., Eibl, D., 2021. Cellular agriculture: opportunities and challenges. Annu. Rev. Food Sci. Technol. 12 (1), 51–73. https://doi.org/10.1146/annurev-food-063020-123940.

Ely, K., Fike, J., 2022. Industrial hemp and hemp byproducts as sustainable feedstuffs in livestock diets. In: Agrawal, D.C., Kumar, R., Dhanasekaran, M. (Eds.), Cannabis/Hemp for Sustainable Agriculture and Materials. Springer, Singapore. https://doi.org/10.1007/978-981-16-8778-5_6.

Farinon, B., Molinari, R., Costantini, L., Merendino, N., 2020. The seed of industrial hemp (Cannabis sativa L.): nutritional quality and potential functionality for human health and nutrition. Nutrients 12 (7), 1935. https://doi.org/10.3390/nu12071935.

Federcanapa, 2025. Vademecum operativo per operatori della filiera canapa – Aggiornato ad aprile 2020 – Alla luce del Decreto Sicurezza e della modifica alla legge 242/2016. https://www.federcanapa.it.

Formici, G., Mancini, M.C., Scaffardi, L. (Eds.), 2026. Cell-Based Meat in the European Union and Beyond: An Interdisciplinary Study. Springer Nature.

Ghenabzia, I., Hemmami, H., Amor, I.B., Zeghoud, S., Seghir, B.B., Hammoudi, R., 2023. Different methods of extraction of bioactive compounds and their effect on biological activity: A review. Int. J. Sec. Metab. 10 (4), 469–494. https://doi.org/10.21448/ijsm.1225936.

Gioria, S., Chassaigne, H., Carpi, D., Parracino, A., Meschini, S., Barboro, P., Rossi, F., 2014. A proteomic approach to investigate AuNPs effects in balb/3T3 cells. Toxicol. Lett. 228 (2), 111–126. https://doi.org/10.1016/j.toxlet.2014.04.016.

Glancy, B., Balaban, R.S., 2021. Energy metabolism design of the striated muscle cell. Physiol. Rev. 101 (4), 1561–1607. https://doi.org/10.1152/physrev.00040.2020.

Halliwell, B., 2003. Oxidative stress in cell culture: an under-appreciated problem? FEBS letters 540 (1-3), 3–6. https://doi.org/10.1016/S0014-5793(03)00235-7.

Hayes, D.P., 2007. Nutritional hormesis. Eur. J. Clin. Nutr. 61 (2), 147–159. https://doi.org/10.1038/sj.ejcn.1602507.

Ho, Y.Y., Lu, H.K., Lim, Z.F.S., Lim, H.W., Ho, Y.S., Ng, S.K., 2021. Applications and analysis of hydrolysates in animal cell culture. Bioresour. Bioprocess. 8 (1), 93. https://doi.org/10.1186/s40643-021-00443-w.

Horne, M. R., 2020. Bast fibres: hemp cultivation and production. Handbook of natural fibres. 163-196. https://doi.org/10.1016/B978-0-12-818398-4.00007-4.

Hubalek, S., Post, M.J., Moutsatsou, P., 2022. Towards resource-efficient and cost-efficient cultured meat. Curr. Opin. Food Sci. 47, 100885. https://doi.org/10.1016/j.cofs.2022.100885.

Jagannathan, L., Cuddapah, S., Costa, M., 2016. Oxidative stress under ambient and physiological oxygen tension in tissue culture. Curr. Pharmacol. Rep. 2 (2), 64–72. https://doi.org/10.1007/s40495-016-0050-5.

Jodynis-Liebert, J., Kujawska, M., 2020. Biphasic dose-response induced by phytochemicals: experimental evidence. J. Clin. Med. 9 (3), 718. https://doi.org/10.3390/jcm9030718.

Karlenius, T.C., Shah, F., Yu, W.C., Hawkes, H.J.K., Tinggi, U., Clarke, F.M., Tonissen, K. F., 2011. The selenium content of cell culture serum influences redox-regulated gene expression. Biotechniques 50 (5), 295–301. https://doi.org/10.2144/000113666.

Lanzoni, D., Bracco, F., Cheli, F., Colosimo, B.M., Moscatelli, D., Baldi, A., Giromini, C., 2022. Biotechnological and technical challenges related to cultured meat production. Appl. Sci. 12 (13), 6771. https://doi.org/10.3390/app12136771.
Lanzoni, D., Skřivanová, E., Rebucci, R., Crotti, A., Baldi, A., Marchetti, L., Giromini, C., 2023. Total phenolic content and antioxidant activity of in vitro digested hemp-based products. Foods 12 (3), 601. https://doi.org/10.3390/foods12030601.
Lanzoni, D., Rebucci, R., Formici, G., Cheli, F., Ragone, G., Baldi, A., Giromini, C., 2024. Cultured meat in the European Union: legislative context and food safety issues. Curr. Res. Food Sci. 100722, 1–16. https://doi.org/10.1016/j.crfs.2024.100722.
Lanzoni, D., Manuguerra, S., Arena, R., Santulli, A., Marchetti, L., Messina, C.M., Giromini, C., 2026. Valorization of hemp, shrimp and blue crab Co-products as novel culture Media ingredients to improve protein quality and antioxidant capacity of cultured meat in cell-based food applications. Foods 15 (2), 352. https://doi.org/10.3390/foods15020352.
Lee, S.Y., Yun, S.H., Jeong, J.W., Kim, J.H., Kim, H.W., Choi, J.S., Hur, S.J., 2022. Review of the current research on fetal bovine serum and the development of cultured meat. Food Sci. Anim. Resour. 42 (5), 775. https://doi.org/10.5851/kosfa.2022.e46.
Levi, S., Yen, F.C., Baruch, L., Machluf, M., 2022. Scaffolding technologies for the engineering of cultured meat: towards a safe, sustainable, and scalable production. Trends Food Sci. Technol. 126, 13–25. https://doi.org/10.1016/j.tifs.2022.05.011.
Liang, P., MacRae, T.H., 1997. Molecular chaperones and the cytoskeleton. J. Cell Sci. 110 (13), 1431–1440. https://doi.org/10.1242/jcs.110.13.1431.
Lindgren, E., Harris, F., Dangour, A.D., Gasparatos, A., Hiramatsu, M., Javadi, F., Haines, A., 2018. Sustainable food systems—A health perspective. Sustain. Sci. 13 (6), 1505–1517. https://doi.org/10.1007/s11625-018-0586-x.
Liu, Y., Gao, A., Wang, T., Zhang, Y., Zhu, G., Ling, S., Du, Y., 2025. Growing meat on autoclaved vegetables with biomimetic stiffness and micro-patterns. Nat. Comm. 16 (1), 161. https://doi.org/10.1038/s41467-024-55048-6.
Mainzer, C., Barrichello, C., Debret, R., Remoué, N., Sigaudo-Roussel, D., Sommer, P., 2014. Insulin–transferrin–selenium as an alternative to foetal serum for epidermal equivalents. Int. J. Cosm. Sci. 36 (5), 427–435. https://doi.org/10.1111/ics.12141.
Mattson, M.P., 2008. Hormesis defined. Ageing Res. Rev. 7 (1), 1–7. https://doi.org/10.1016/j.arr.2007.08.007.
Milanesi, L.M., Vasconsuelo, A.A., Pronsato, L., Frattini, N.M., Blanco, N.O., 2024. Indole family and neomycin sulfate: inductors of differentiation in C2C12 and RD cell lines. J Cell Signal 5 (4), 195–207.
Mitsuishi, M., Miyashita, K., Muraki, A., Itoh, H., 2009. Angiotensin II reduces mitochondrial content in skeletal muscle and affects glycemic control. Diabetes 58 (3), 710–717. https://doi.org/10.2337/db08-0949.
Neinast, M., Murashige, D., Arany, Z., 2019. Branched chain amino acids. Ann. Rev. Physiol. 81 (1), 139–164. https://doi.org/10.1146/annurev-physiol-020518-114455.
Nikawa, T., Ulla, A., Sakakibara, I., 2021. Polyphenols and their effects on muscle atrophy and muscle health. Molecules 26 (16), 4887. https://doi.org/10.3390/molecules26164887.
Post, M.J., 2012. Cultured meat from stem cells: challenges and prospects. Meat sci 92 (3), 297–301. https://doi.org/10.1016/j.meatsci.2012.04.008.
Prieto, J.M., 2012. Procedure: preparation of DPPH Radical, and antioxidant scavenging assay. DPPH Microplate protocol 7–9.
Qin, D., Bo, W., Zheng, X., Hao, Y., Li, B., Zheng, J., Liang, G., 2022. DFBP: a comprehensive database of food-derived bioactive peptides for peptidomics research. Bioinform 38 (12), 3275–3280. https://doi.org/10.1093/bioinformatics/btac323.
Sachse, A., Wolf, G., 2007. Angiotensin II–induced reactive oxygen species and the kidney. J. Am. Soc. Nephrol. 18 (9), 2439–2446. https://doi.org/10.1681/ASN.2007020149.
Sherman, B.T., Hao, M., Qiu, J., Jiao, X., Baseler, M.W., Lane, H.C., Chang, W., 2022. DAVID: a web server for functional enrichment analysis and functional annotation of gene lists (2021 update). Nucleic Acids Res 50 (W1), W216–W221. https://doi.org/10.1093/nar/gkac194.
Simonic, T., Duga, S., Negri, A., Tedeschi, G., Malcovati, M., Tenchini, M.L., Ronchi, S., 1997. cDNA cloning and expression of the flavoprotein D-aspartate oxidase from bovine kidney cortex. Biochem. J. 322 (3), 729–735. https://doi.org/10.1042/bj3220729.
Singh, S., Chaudhary, K., Dhanda, S.K., Bhalla, S., Usmani, S.S., Gautam, A., Raghava, G. P., 2016. SATPdb: a database of structurally annotated therapeutic peptides. Nucleic Acids Res 44 (D1), D1119–D1126. https://doi.org/10.1093/nar/gkv1114.
Stacey, D.W., 2003. Cyclin D1 serves as a cell cycle regulatory switch in actively proliferating cells. Curr. Opin. Cell Biol. 15 (2), 158–163. https://doi.org/10.1016/S0955-0674(03)00008-5.
Stout, A.J., Rittenberg, M.L., Shub, M., Saad, M.K., Mirliani, A.B., Dolgin, J., Kaplan, D. L., 2023. A Beefy-R culture medium: replacing albumin with rapeseed protein isolates. Biomaterials 296, 122092. https://doi.org/10.1016/j.biomaterials.2023.122092.
Straus, D.S., 1981. Effects of insulin on cellular growth and proliferation. Life Sci 29 (21), 2131–2139. https://doi.org/10.1016/0024-3205(81)90482-3.
Sundaram, T.S., Giromini, C., Rebucci, R., Lanzoni, D., Petrosillo, E., Baldi, A., Cheli, F., 2025. Milk whey as a sustainable alternative growth supplement to fetal bovine serum in muscle cell culture. J. Dairy Sci. 4749–4769. https://doi.org/10.3168/jds.2024-2544.
Tavares, T.G., Contreras, M.D.M., Amorim, M., Martín-Álvarez, P.J., Pintado, M.E., Recio, I., Malcata, F.X., 2011. Optimisation, by response surface methodology, of degree of hydrolysis and antioxidant and ACE-inhibitory activities of whey protein hydrolysates obtained with cardoon extract. Int. Dairy J. 21 (12), 926–933. https://doi.org/10.1016/j.idairyj.2011.05.013.
Van Der Valk, J., Bieback, K., Buta, C., Cochrane, B., Dirks, W., Fu, J., Gstraunthaler, G., 2018. Fetal bovine serum (FBS): past–present–future. Altex 35 (1), 1–20.
Vermeulen, S.J., Campbell, B.M., Ingram, J.S., 2012. Climate change and food systems. Ann. Rev. Environ. Res. 37, 195–222. https://doi.org/10.1146/annurev-environ-020411-130608.
World Health Organization, 2023. Food Safety Aspects of Cell-Based Food. World Health Organization.
Yoshida, T., Galvez, S., Tiwari, S., Rezk, B.M., Semprun-Prieto, L., Higashi, Y., Delafontaine, P., 2013. Angiotensin II inhibits satellite cell proliferation and prevents skeletal muscle regeneration. J. Biol. Chem. 288 (33), 23823–23832. https://doi.org/10.1074/jbc.M112.449074.
Zambonelli, C., Morandi, P., Vanoni, M.A., Tedeschi, G., Servi, S., Curti, B., Monti, D., 2003. Cloning and expression in Escherichia coli of the gene encoding streptomyces PMF PLD, a phospholipase D with high transphosphatidylation activity. Enzyme Microb. Technol. 33 (5), 676–688. https://doi.org/10.1016/S0141-0229(03)00190-X, 33(5), 676-688.
Zanderigo, G., Bracco, F., Semeraro, Q., Colosimo, B.M., 2023. In-situ printability maps (IPM): a new approach for in-situ printability assessment with application to extrusion-based bioprinting. Bioprinting 36, e00320. https://doi.org/10.1016/j.bprint.2023.e00320.
Zhu, Y., Wang, K., Jia, X., Fu, C., Yu, H., Wang, Y., 2024. Antioxidant peptides, the guardian of life from oxidative stress. Med. Res. Rev. 44 (1), 275–364. https://doi.org/10.1002/med.21986.

Further readings

Cabello-Verrugio, C., Acuña, M.J., Morales, M.G., Becerra, A., Simon, F., Brandan, E., 2011. Fibrotic response induced by angiotensin-II requires NAD (P) H oxidase-induced reactive oxygen species (ROS) in skeletal muscle cells. Biochem. Biophys. Res. Commun. 410 (3), 665–670. https://doi.org/10.1016/j.bbrc.2011.06.051.
Post, M.J., Levenberg, S., Kaplan, D.L., Genovese, N., Fu, J., Bryant, C.J., Moutsatsou, P., 2020. Scientific, sustainability and regulatory challenges of cultured meat. Nature food 1 (7), 403–415. https://doi.org/10.1038/s43016-020-0112-z.
Sinclair, J.R., 2019. Importance of a one health approach in advancing global health security and the Sustainable Development Goals. Rev. Sci. Tech. 38 (1), 145–154. https://doi.org/10.20506/rst.38.1.2949.